FTIR and XRD Characterization of the Cements Available in Commercial Market of Nepal

ABSTRACT:
In the engineering material characterizations and analyticaldomains where the specific physicochemical properties of the materials are probed through various sophisticated instrumental tools and techniques,the XRD and FTIR spectroscopy stand as the standalone applications as the former discloses the crystallographic structure, crystallite/grain sizes, and the chemical compositionsof the specific materials nondestructivelywhile the latter reveals details about theIR active vibrations modes of each covalent bond of their chemical constituents. In the present studies, we employ both of these techniques, and characterize the specifically selected variable manufactured ready-to-use dry OPC type cements available in the commercial markets of Nepal. The former technique derived the specific 2θ value deterministic for identifying the closely packed interatomic layers with the significant levels of $CaCO_3$, $Ca(OH)_2$, and arsenic As^{5+} based AsO_4^{3-}unit bearing crystalline phases in each samples. The calculated crystallite sizesof themare foundas equal as that reported for the calcite based OPC cements, and are directly adopted to depict their utmost intermixing propensities with the carbon dust and hence, act as the most potential evidence of unlocking the possibility of inventing cement-carbon supercapacitors and conductive devices, and of speculating their distinguishable hydration rates and setting times. And, the latter technique produced intense IR active bands in the designated wave number regions are used to confirm their silicate (SiO_4^{2-}) tetrahedra, amorphous $CaCO_3$phases &the CO_3^{2-}unit holding chemical constituents, $2CaO.SiO_2$ and $3CaO.SiO_2$ type chemical compounds explicitly. The presence of diffused type IR bands specific to the Al_2O_3based chemical compounds signified that all of them containssignificant levels of the alumina based hardening elements, but the complete absence of the peak typical to theMg–O signified that none of them containsmagnesia. The similar analyses of the IR bands further reveal that none of them possessesheavy and active type $CaCO_3$, but have trace amounts of the AsO_4^{3-} based chemical compounds as predicted by the XRD. The intensive peak area and the depth intensity studies of the designated IR bands speculate the dissimilar quantitative proportions and percentage compositions of these chemical constituentsin them. The authors believe that the general results presented herewith illuminate the fundamental chemical constituents to be incorporated compulsorily into the OPC type cements so that they function normally and exhibit good cementitious abilities.

KEYWORDS: OPC Cements, Crystallite/Grain Sizes, Health Hazards, Calcite/Alumina/Magnesia

1. INTRODUCTION

Among the various kinds of civil engineering materials, cement is one of the mostly used chemical substancesworldwide as a major constructive material offering exceptional binding abilities to other different typesreinforced materials with exhibiting remarkable setting, hardening, and adhering propensities. In engineering field, it is basically used in mortar for plastering, hardening, masonry works, pointing, shaping, etc. because of possessing rapidhydration and setting times/rates, exceptional durability &material strength, and imparting long-lasting power to the wide arrays of engineering structures[1–3].It is frequently used as a primary material for developing joints, drains&pipes, sealants, laying the floors &roofs, and constructing the lintels, beams, stairs, pillars, etc. plus for constructing the basement foundations, and stabilizing the engineering structures such as bridges, culverts, dams, tunnels, lighthouses, etc. at several geologically challenging areas. Mostly, it is selectively employed in developing a hard surface over the vulnerable engineering structures that feel extremely unsafe from the various destructive weather scenarios, and many other specific chemical attacks [4,5]. All these exceptional applicationsof the cement as afundamental cornerstone, and its massive utilizations in the field of diverse engineering endeavors are actually governed by its own exceptional structural stability and long-lasting endurance, severe materials binding abilities, profound adaptability, and extensive durability [1–6]. And, all those critical roles and functions plus the overall outcome and performance that make the cement an ideal engineering material are led by its unique chemical compositions (hereafter, chemical constituents) comprising with limestone ($CaCO_3$), clay (SiO_2 and Al_2O_3), gypsum ($CaSO_4 \cdot 2H_2O$), and many other predominant chemical compounds such as dicalcium silicate ($2CaO.\ SiO_2$; hereafter C_2S), tricalcium silicate ($3CaO.\ SiO_2$; hereafter C_3S), tricalcium aluminate ($3CaO.Al_2O_3$; hereafter C_3A), and tetracalciumaluminoferrite($4CaO.\ Al_2O_3.\ Fe_2O_3$; hereafter C_4AF) formed through the respective

chemical reactions of the clinker: $CaCO_3 \rightarrow CaO + CO_2$; $SiO_2 + 2CaO \rightarrow 2C_2S$; $CaO + 2CaO.SiO_2 \rightarrow 3C_3S$; $Al_2O_3 + 3CaO \rightarrow 3C_3A$; $4CaO + Al_2O_3.Fe_2O_3 \rightarrow 4C_4AF$.At the time of mixing cements with water uniformly (water cement w/c ratio = 0.3–0.6by mass), these chemical constituents undergo the hydration type chemical processesthat resultto the formation of robust type hydrated matrix (calcium silicate hydrate (C–S–H gel); a nano sized material) which not only contributes to glue the aggregates/cement particles effectively and enhances the plastering/placing tendenciesof the cements but also determines their characteristic features owing to enrich adhering abilities such as setting time, strength advancement, &resilience against environmental influences, hardening and durability, wearing/tearing resistance,etc.[6(a)]. The C_3S and C_2S chemical components of the cement, however, provide early and late strengths to the concrete type robust material respectively [6(b)].

While referring to the prevailing consumption rates of the engineering materials worldwide in terms of their extensive employments, critical significance in the construction sectors,and primary characteristic properties, the cement only has this rate more than 4 billion metric tonnes/year [2]. In the context of Nepal, the annual per capita cement consumption is303kg; a rate higher than in India (195kg), and lesser than in China (1,716kg)&even Bhutan (734kg) [7], and is already predicted industrially as 26million tons/year by the end of the fiscal year 2024–2025. This sudden surge in demand of the cement nationwide is attributed to the rapid urbanization pace, construction boom ofthe commercial structures, and undertaking of various mega national pride projects across the country[8].Currently, the total installed and the genuinely operated capacity of the cement industriesin Nepal produce collectively4,225tons of cement/day; 2,783tons by foreign investment factories, 820tons by state-owned factories, and 622tons by privately run factories. It means the nationwide full production capacityof the cement is reached

to the level of 15 million metric tons/year, but its actual integrative production rate stands at 7.49 million metric tons/yearwhile the present nationwide consumption demand rate is at 9.05 million metric tons/year. In terms of the investments injected by the foreign (NRs.56.97 billion) and Nepali citizens (NRs.122.33 billion), the remarkable progress and the advancement in national cement production rate is achieved. In terms of utilizing the net amount of limestones (foreign owned factories: 0.99tons on average; state-owned factories: 1.45tons)in producing 1tonne of cement, and the total amount of clinkers consumed per year (7 million tons/year) [8(b)], the foreign invested factories are recognized as thetechnologically modernized, functionally efficient, operationally potent, productionally more yet diverse in quantitative scale, and brandwiseextra unique.Therefore, the mostly available cement products in the commercial market of Nepal are foreign run factories made, and the tentative cost of each 50kg sack produced by them including those manufactured by the state-owned factories lies in the range of NRs 700 to NRs1100. In regard to the cement brands and the production technologies associated with them plus the public desires and needs, the four topmost predominant Nepal-made branded cements are Hongshi; a foreign invested, and Chaudhary Group (CG), Jagadamba&Sarbottam; the privately owned factories.As a whole, the domestic market in Nepal even though offers a wide range cement products with variable efficiencies, and construction abilitiesbecause of which the concerned stakeholders are getting enough chances to choose the selective brands aligned best to their preferences and needs, the full nationwide demands and needsplus consumption rates as per the consumers' and construction professionals' specific projectsare notcompletely fulfilled yet. To ensure the timely address of this most probable market shortage of the cements, and to regularize/mobilize their brandsnationally and internationally, the government of Nepal on the one hand imports significant quantity of the

branded cements from India, Germany, and Austria (the 123rdlargest importer in the world [10]), and on the other hand it exports state-made branded cements to the neighboring country such as India in substantial amounts (in the last seven months of the fiscal year 2023–2024, the cements worth around NRs 170 million is exported) [11]. These quantitative figures and the existing nationwide scenariosas a whole underscore the requirements of installing state-of-art cement production technologies, establishing the additional industrial plants, operating the existing plants in a full-fledged condition, etc. nationwide so that the increasing rate of cement consumption trends, the constantdemands of them in the commercial Nepalese markets, and their massive uses in various engineering sectors can be promptly addressed [9].

Unfortunately, the existing cement industries in Nepal are facingseveral challenges out of which the timely non-disruptive supply of the clinkerfrom the foreign lands is the major ones despite the government's initiations to mitigate the risks associated with it either by encouraging the local clinker productions, establishing the large integrated clinker production plants, regulating the supply of promising type clinker based ingredients, and raw materials, installing the latest yet sophisticated industrial technologies or by implementing the benchmark manufacturing and products distributing policies [9–11]. Additionally, the shortage of the skilled workforce for the specific Researches& Developments (R & D), and the allocation of the inadequate budgetto the R & D sectors are further worsening the industrial pace of the development, advancement, improvement, and innovations of the esteemed products day by day. The better yet innovative cement products, internationally recognized types,technologically potent, and the chemical–constitutionally appropriate cement items can only be expected/delivered to the Nepalese commercial markets if the foreign installed, state–owned, and privately financed factories offer a large scale research opportunities and instrumental

characterization facilities, allocate enough R & D budgets, provide research internships facilities, and extend innovation &designation platforms intensively. In this context, the current research workaimed mainly at performing in-depth instrumental (X–ray diffraction (hereafter, XRD) and Fourier transform infrared (hereafter, FTIR))characterizations of the cements and their crystallites, grains, and particles plus their chemical constituents such as carcinogenic components, alumina, silica, magnesium oxide, sulfates, & their composites and investigating their explicit decisiveroles in enhancing quality of the cement and cement based products is indispensable.Beside this, the present research focusing into the qualitative comparisons of the basic chemical constituents present in the different brands (CG, Hongshi, Sarbottam, Jagadamba) of the cement samples selected in this studypreferentially which in fact make them of good quality&high standard, characteristically desirable & demandable in the commercial markets with some unique fames may add valuableinputs to the R & D sectors of the cement and cement based material industries.Towards health, environmental and engineering perspectives, this research work would be highly beneficial in terms of identifying the pollution causing grain size ranges and cement particulates, and adopting some basic safety precautions that need to be incorporated into the national production/construction policy with health, safety, and accidental prevention schemes so that the site engineers and other production/ construction crew memberswon't experience a sudden accidental, occupational, and injury health hazards directly. More importantly, this work can be taken as a doctrine document and a quite essential yet mandatory guideline drafttowards the consistent quality control & dependable cement products, constant monitoring&regulation of the manufacturers' policies, central inspection of the specific cement samples and their qualitative performance evaluation, precise material optimization and advancement of the high–performance concretes, exact identifications of any undesirable and

quality degrading phases of the cementin quantitative/qualitative scales, etc. To the knowledge of the present authors, the related flavors based on the instrumental characterizations of the Nepal–made cements are rarely available. In the views of all these potential attributes, this research work may serve asa stepping-stone towards standardizing the national industrial manufacturing policies and production guidelines, and maintaining the standard norms of the cements produced nationwide. This research paper is structured as: Materials & Methods in section 2, Results &Discussions in section 3, and Summary &Conclusions in section 4.

2. MATERIALS AND METHODS

2.1 Collection of the Selected Sample Specimens

As per the need of this instrumental (FTIR and XRD) analytical study of the ordinary Portland cement (OPC) samples available yet publicly desirable at the commercial market of Kathmandu valley, we procured and collected four distinct OPC cement samples (CG, Hongshi, Sarbottam, Jagadamba) directly from their respective depots where the large quantities of them are stored in High-Density Polyethylene (HDPE) 50 kg sacs, and are dispatched to the construction sites as per their prompt demands. We randomly named them as CS1, CS2, CS3, and CS4 in order to maintain their confidentiality including designated manufacturers, commercially known brand names, R & D characteristic features, and the overall industrial cement producing policies. Each sample holder (polyethylene bottles) was made air–tight,and sealed with the aluminum foil layered stoppers just to protect them from humid weather exposures, and to maintain their powdered forms with characteristic physicochemical properties as shown in Figure 1.The selection of every cement sampleswas meticulously done based on their extraordinary performances in advancing and strengthening the commercial engineering structures, and their peak demands in the Nepalese markets. Additionally, the (a) fundamentalchemical

constituentswith variable compositions, (b) compressive and adhering strengths, hydrating propensities, and setting/placingabilities with remarkable durability, (c) modern manufacturing procedures with eco-friendly technology, (d) pre- &post- treatment requirementsof the cemented sites, (e) popularity and market availability in the Kathmandu Valley, etc.[9] of each of the

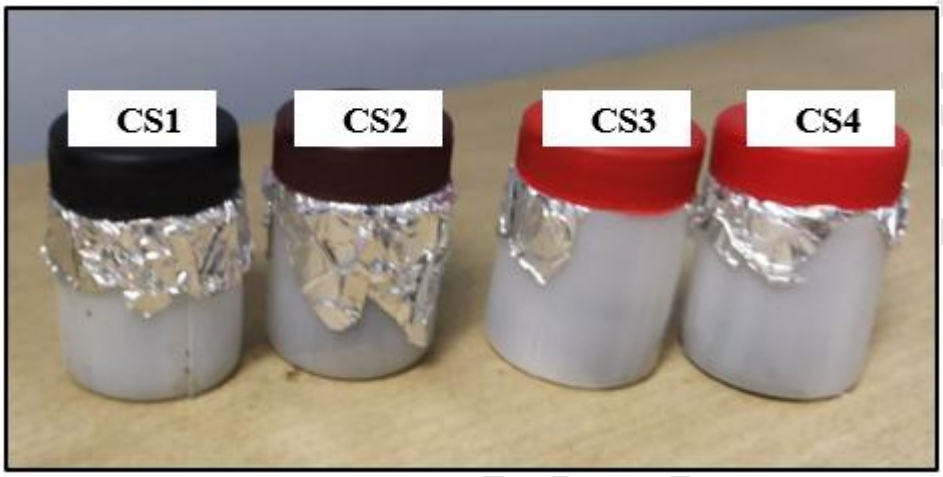

Figure 1. The four different sample holders (polyethylene bottles) containing the experimental specimens of cement samples CS1, CS2, CS3, and CS4. The aluminum foil layered stoppers are used securely for making each of them perfectly air-tight, and sealed.

samples were considered genuinely in the course of their explicit selections and declarations as the experimental specimens of this study.

2.2 Measurements of the XRD Diffractograms

Since the specific institution where the authors are affiliated with is not equipped with the X-Ray diffraction facility needful to this study, we straightforward submitted each of the samples (sealed as in Figure 1) to Nepal Academy of Science and Technology (NAST); a government funded institution dedicated fully to advance the research and development sectors nationwide [12]. As per its policy, the XRD facility is made available commercially to the academic and industrial R & D sectors, and the prompt measurement of the specific samples is carried out as

per the requirements of the customers with the acceptance of nominal service charges. The XRD instrument owned by it, and used herewith for the characterizationsof each cement sample CS1, CS2, CS3, CS4 was bench-top diffractometer BRUKER D2 PHASER which normally florescence under Copper X−rays. All the XRD patterns of each cement sample were obtained in the 2θangular range of 10–90°, a step size of angular increment 0.02°, and a material scanningrate of 0.5°/min. Prior to that, the calibrations and standardizations of the XRD machine were carried out as per the instructions listed in the operational manual prescribed by the manufacturer [13]. All the concerned raw XRD datasets of each samplespecimen weredirectly plotted as a diffractogram for the subsequent analyses and interpretations.

2.3 Measurements of theFourier Transform Infrared (FTIR) Spectrograms

Alike to the XRD facility, the institution where the authors are affiliated with is not equipped with the Fourier Transform Infrared (FTIR) spectroscopy tools, and meanwhile, the FTIR facility offered by the NAST was not in the operational condition due to some unavoidable circumstances. Therefore, for the FTIR measurements, we specifically submitted each of the cement samples in powdered form (Figure 1) tothe Research Centre for Applied Science and Technology (RECAST); an organizationowned by Tribhuvan University, Nepal for promoting the applied science disciplinesin strengtheningthe academic and industrial pace of developments [14]. The analytical FTIR spectrometer hosted by it, and utilized herewith is Shimadzu IRAffinity−1S (S. No. AZ1965904022); a high precision equipment ideal especially for the quantitative spectroscopy analyses. Prior to the specific measurements, the instrument was at first calibrated at ambient air conditions, and its in-built precisionlevel was standardized as per the operational manual made available by the manufacturer elsewhere [15]. Subsequently, a trace amount of the cement sample in the powdered form was carefully placed in the designated

sample compartment of the instrumentjust to ensure the instrumental stabilitythroughout the measurement procedures of the spectral patterns.After this genuine calibrations, the actual measurement process of the samples was initialized, and the specific interferogram sketched for every sample specimenswith the concerned raw datasets (intensity of light over time) was recorded explicitly.By means of Fourier transformation, every interferograms were converted into the infrared (IR) spectrum; a graphical sketch depicting the relationships between the intensity (% transmission of the sample)of IR absorbance against the wave numbers (cm^{-1}).While measuring the FTIR spectra, the spectral range of 4000–400 cm^{-1}, featuring a resolution of 4 cm^{-1} and an average of 50 scans/sample was implementedinstrumentally.

2.4 XRD–Peak Fittings with *Gaussian* Convolution

Based on the powder characterization skills of the XRD tools, and the principalobjectives set to the present study, we rigorously analyzed the XRD patterns of each cement sample explicitly. In the course of analyzing the same, we at first identified the most intense XRD peak of each cement sample at the specific diffraction angle (2θ), and retrieved the required datasets explicitly followed by their subsequent subjection to the *Gaussian* convolutions for peak fitting. The specific Cartesian coordinates assigned for displaying theparticular *Gaussian* convolutionsin three dimensional space were programmatically created, and the required manipulation was carried out based on the need of peak fitting techniques. The controlling parameters such as peak height (H), peak width (W), and full width at half maximum (herewith, FWHM (β)) were determined based on the live simulations performed in the Microsoft Excel spreadsheet platform.The specific 2θ value recorded for the most intense XRD peak of each sample specimen was used to find out the interlayer distance d(distance between the crystalline lattice planes) by employing the Bragg's law of diffraction formulated in Eq. 1.

$n\lambda = 2d\ sin(\theta)$ (1)

Where;

n = integer for order of diffraction.

λ = wavelength of the incident X–ray ($\lambda = 1.54$ Å[16, 17])

θ= angle of incidence($\theta = 2\theta/2$)

And, the FWHM value $\beta$of each sample was used to estimate the specific crystallite size$L$by employing the mathematical relation (Scherrer's formula) shown in Eq. 2

$L = (K \times \lambda) / (\beta \times cos(\theta))$ (2)

Where;

K = Scherrer's constant.

The numeral value for the constant K was actually determined using the relation shown in Eq. 3; a specially recommended formula for the cases where the (a) FWHM value is determined through the *Gaussian* peak fitting technique, and (b) material is mostly made up of spherical particulates (in this case, the specimen cement samples are those typeengineering materials that arecomprised with the maximum proportion of spherical type fly ash particulates [18, 19]).

$K = 2\sqrt{(\ln 2)/\pi} \cong 0.9394$ [20, 21] (3)

Each specific value of L determined for the samples CS1, CS2, CS3, CS4, and their respective d values were substituted in Eq. 4, and determined their number of parallel interatomic planes$m$ stacked one over the other periodically by maintaining the definite gap$d$in their crystalline phases.

$m = \frac{L}{d}$ (4)

3. RESULTS AND DISCUSSIONS

3.1 Interpretations of the XRD Diffractograms

In the qualitative and quantitative solid state samples characterizations, and the specific compositional analyses,the powder XRD instrumental procedure is well recognized technique and the most esteemed analytical tool worldwide not only due to its nondestructive nature but also its fingerprint basis of identifying crystallite phases and sizes accurately. The several unique aspects of its morphological analytical perspectivesadd substantial values to its rational applications in wide ranged materials [20]. In fact, both of its qualitative and quantitative analytical schemes are governed by the Bragg's law of diffraction which relates the interlayer distance (d) of the crystalline solid state materials with the specific angle of diffraction (θ) (Eq. 1), and are based on the principle:"every solid state materials or crystalline compoundspossess unique solid state lattice giving distinctive X–ray diffraction patterns so that the inter layer distance$d$between the crystalline lattice planes of each material can be identified accurately just by the precise scaling oftheir XRD diffractograms with the standard pre-establisheddatabases" [20, 21]. Being the cement and cement based materials solid state crystalline phases type comprising with the characteristic clinker phases of their manufacturing stages, the powder XRD instrumental technique is equally suitable to probe their wide ranged specimensmore especially in the light of in–depth material characterizations, interatomic layer distances$d$,and the quantitative sizes of thecrystallites, grains, and the particles as a whole [22,23, 24]. Additionally, this technique is more significantly applicable to access the purity of the cement samplesvia the closed inspection of theirX–ray diffraction patterns bytakingintoconsiderationtheproportionsandcompositions of their impurities [23]. Herewith, the XRD investigations of the four preferentially selected different OPC cement samplesnamed randomly with CS1, CS2, CS3, and CS4 (Figure 1) that are manufactured and made available to the public markets by the four different industrial plants arecarried out explicitly, and inspected

their respective diffractograms with specific spectral patterns prior to characterizing their

crystalliteand grains morphology. The concerned OPPXRD–1: BRUKER D2 PHASER

diffractometer produced XRD patterns ofthe respective sample specimens are displayed in

Figure 2 and Figure 3 where themost intense spectral peak assigned to each sample specimen is

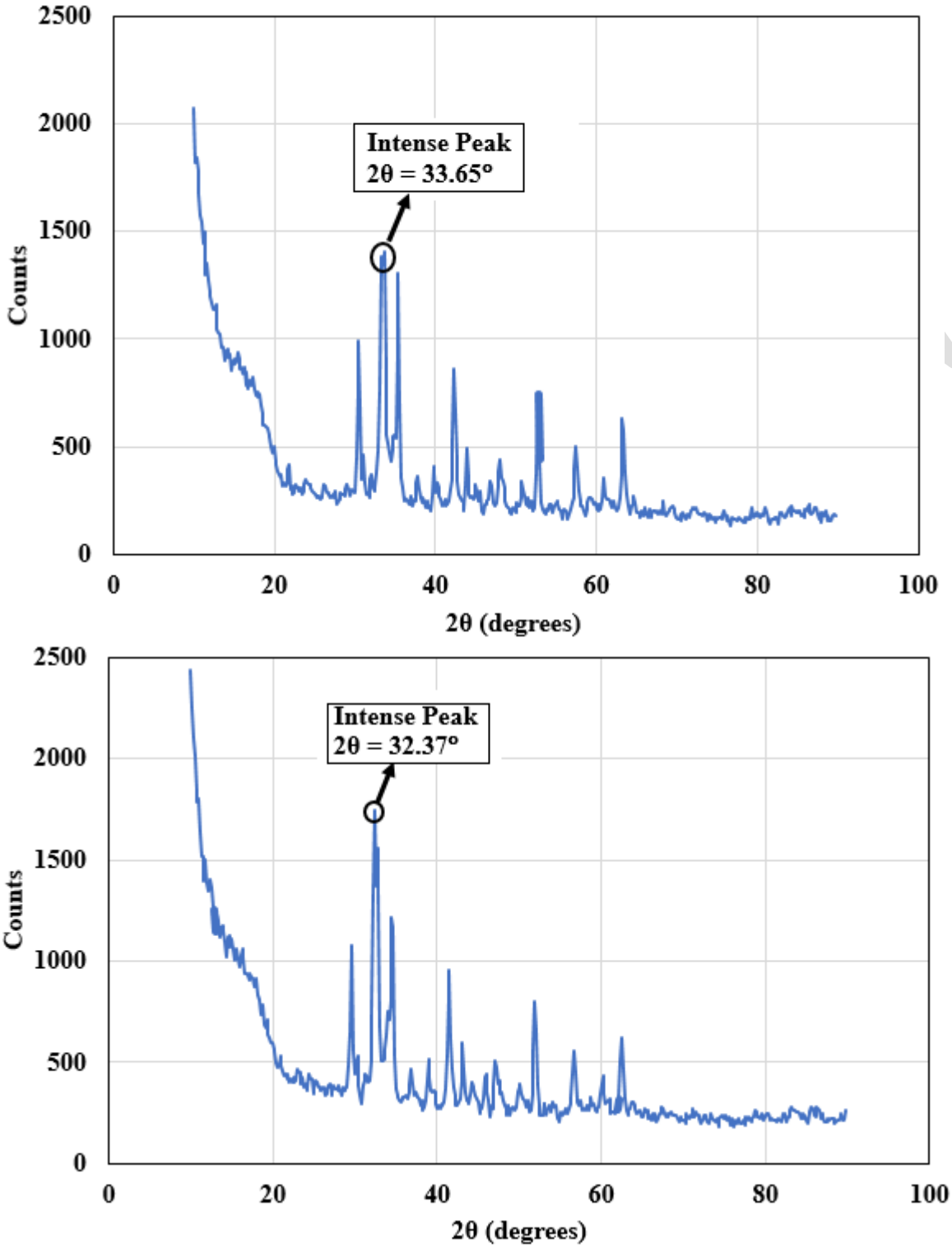

Figure 2. The XRD diffractograms for the cement samples **(A)** CS1, and **(B)** CS2. The most intense peaks assigned to each sample are marked with their 2θ values in degrees.

marked with the2θ value in degree.The relatively low heights peaks are ignored and not

characterized them herewith as they lie beyond the scopes of this research work, and do not play significant roles in estimating crystallite sizes and thickness.In average, the most intense spectral peak assigned to each of the samples is appeared almost at $2\theta = 33°$; a fingerprint peak for the $CaCO_3$ phase of the cements ($CaCO_3$ phase is present from the manufacturing stages of the cements, and few amount of it is added lately due to atmospheric CO_2 attack in humid conditions). More particularly, the intense spectral peak for the sample CS1 is appeared at $2\theta = 33.65821°$, that for the rest of the samples CS2, CS3, and CS4 are stood at the baseline of $2\theta = 32.37949°$, $2\theta = 32.53933°$, and$2\theta = 32.69917°$ respectively as can be scaled in the respective figures (Figure 2 and Figure 3). The specific datasets that includethe concerned XRD countsof each of these intense peaks and their specific 2θangular values are fitted with the *Gaussian* convolutions (Figure 4, and Figure 5), and determined their respective FWHM (β) values as 0.566137°, 0.549486°, 0.249766°, and 0.266417°as listed in Table 1. By employing the Bragg's law with the mathematical formulationsshown in Eq. 1, the concerned interlayer (atomic layers) distance d of each of the sample specimens is estimated by substituting the specific values of the XRD predicted θ(Table 1) assigned to their most intense peaks, order of diffraction ($n = 1$), and wavelength of the X–ray(λ= 1.54 Å) as listed in third column of Table 1. In principle, the interlayer distance d always measures the basal spacing and the gap between any two consecutive interatomic planes of the solid-state cement material phases, and it acts as a deterministic descriptor for inspecting the packing tendencies of the basal planes of the crystals. Based on this reference, theXRD predicted dissimilar distance values d between any two consecutive atomic layers of the four different solid state cement samples indicate their distinguishable interlayer packing and crystallinity. More specifically, the cement sample CS1 is found to possess the smallest d value(d = 2.7Å) among the four sample specimens; suggesting

Table 1. The Bragg's law and Scherrer's formula derived interlayer distance d, and crystallite size D of four different cement samples CS1, CS2, CS3, and CS4.

Cement samples	XRD Peak Positions		Interlayer Distance (d) (nm)	FWHM (β) (°)	Crystallite Size L (nm)		No. of parallel planes m
	2θ	θ			L	Average L	

itscrystalline phases more closely packed interatomic layers. And, the remaining three CS2, CS3, and CS4 specimens are observed to have the d value in the range of d = 2.8Å; confirming their crystalline phases comprisingwith the comparable interlayer packing ratios. Interestingly, all those interlayer distance d values determined herewith for four different ordinary Portland type cement samplesthat were collected directly from their High–Density Polyethylene (HDPE) 50 Kg sacslie in the aggregable range to that reported previously elsewhere [24] for the As^{5+}–bearing oxyanions (AsO_4^{3-}) Portland cement type–V(d= 2.8Å to 3.0 Å) of 10–day– and 1–month–old samples. It exemplified that all the four different cement samples we analyzed herewithmay contain the phases of$Ca(OH)_2$ (d = 2.7Å), $CaCO_3$ (d = 2.9Å),$CaHAsO_4.2H_2O$ (d = 2.9Å),$CaH_4(AsO_4)_2.2H_2O$ (d = 2.2Å) and $Ca_3(AsO_4)_2$ (d = 2.9Å)type chemical compounds as their stabilization/solidification (S/S) matrix constituents[25].Thus speculated As^{5+}–bearing chemical compounds in the current OPC type cement samples actually make themselves suitable for immobilizing As^{5+}bearing wastes and for mitigating the environmental hazards including the effective treatments of the industrial wastes containing toxic metals. It supports the existing practices of employing cements in treating metal ions contaminated industrial effluents from long time before [26].

CS1	33.65821	16.829106	0.2660628	0.56613	15.30	24.51	58
CS2	32.37949	16.18974	0.2762721	0.54948	15.71		57
CS3	32.53933	16.26966	0.2749514	0.24976	34.58		126
CS4	32.69917	16.34958	0.2736438	0.26641	32.44		119

Alike to these interlayer distance *d*based interpretations associated with the Bragg's law

of diffractions, the closely related yet more rigorous material and crystallite size L plus the grain

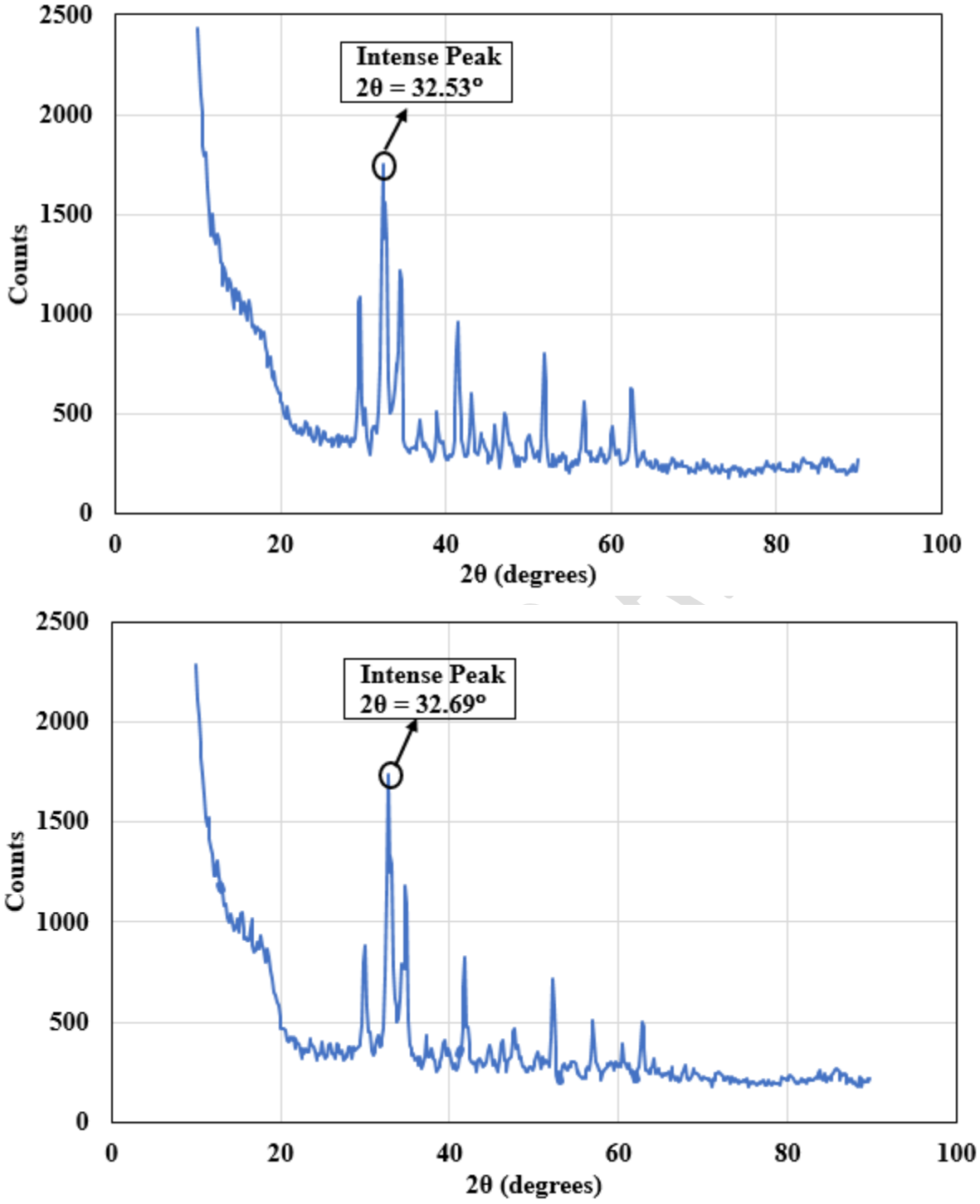

Figure 3. The XRD diffractograms for the cement samples **(A)**CS3, and **(B)**CS4. The most intense peaks assigned to each sample are marked with their 2θ values in degrees.

size analyses of each of the cement samples can be carried out by employing the Scherrer's formula formulated in Eq. 2 [20, 21].While substituting the specific values of the Scherrer's

constant K derived from Eq. 3, the FWHM (β) derived from *Gaussian* convolution fitting techniques, and the angle θassigned to the most intense peakderived throughthe XRD in Eq. 2,the crystallite size L of each of the cement samples is found to be in the range of 24.51nmin average (Table 1). This average crystallite size and thickness lies in the range of the crystallite sizes of the normal standard OPC cements whose L value is reported in between2 nm to 80 nm based on their nanosized comprising boehmite alumina modified with SiO_2, CaO, and MgOcompounds [27].Moreparticularly,the samples CS1 (L =15.30 nm) and CS2 (L =15.71 nm) are characterized with the L valuesalmost half to those determined for the samples CS3 (L=34.58 nm) and CS4 (L=32.44 nm). Interestingly, the first two samples are identified as those whose L values are as equal as that reported for the $MnFe_2O_4$ spinel nanoparticles based OPC cement (L = 16 nm) [28], and the latter two are categorized as those whose L values are as equal as that reported for the calcite based OPC cement (d= 3.03Å, L = 30 nm) [29]. The precise physical meaning of L actually stands for the size of the single crystal of each cement sample which in fact decides the grain size or the maximum proportionsizes of the particlesdistributed throughout the materials. And, in the growth and development processes of the grains, the crystallites gather closely in the definite matrix form kinetically and attain the bigger sized particles [20, 21].This phenomena of agglomeration play predominant roles more especially in the cement and cement based materials in specifying their packing tendencies and void volume, weight and density of the materials, water absorbing propensities, and the plastering/adhering/setting/curing/post–treatment frequencies. Based on these pre-established facts, almost half in sizes of the crystallites$L$ of the first two cement samples CS1 and CS2tentatively reflect that they grow and agglomerate each other by producing relatively smaller particle or grain sizes than that of the latter two samples CS3 and CS4 even though the nature of

the agglomeration and amalgamation of the crystallites is dependent with the external

temperatures, humidity, packing densities, and more importantly the particles morphology [30,

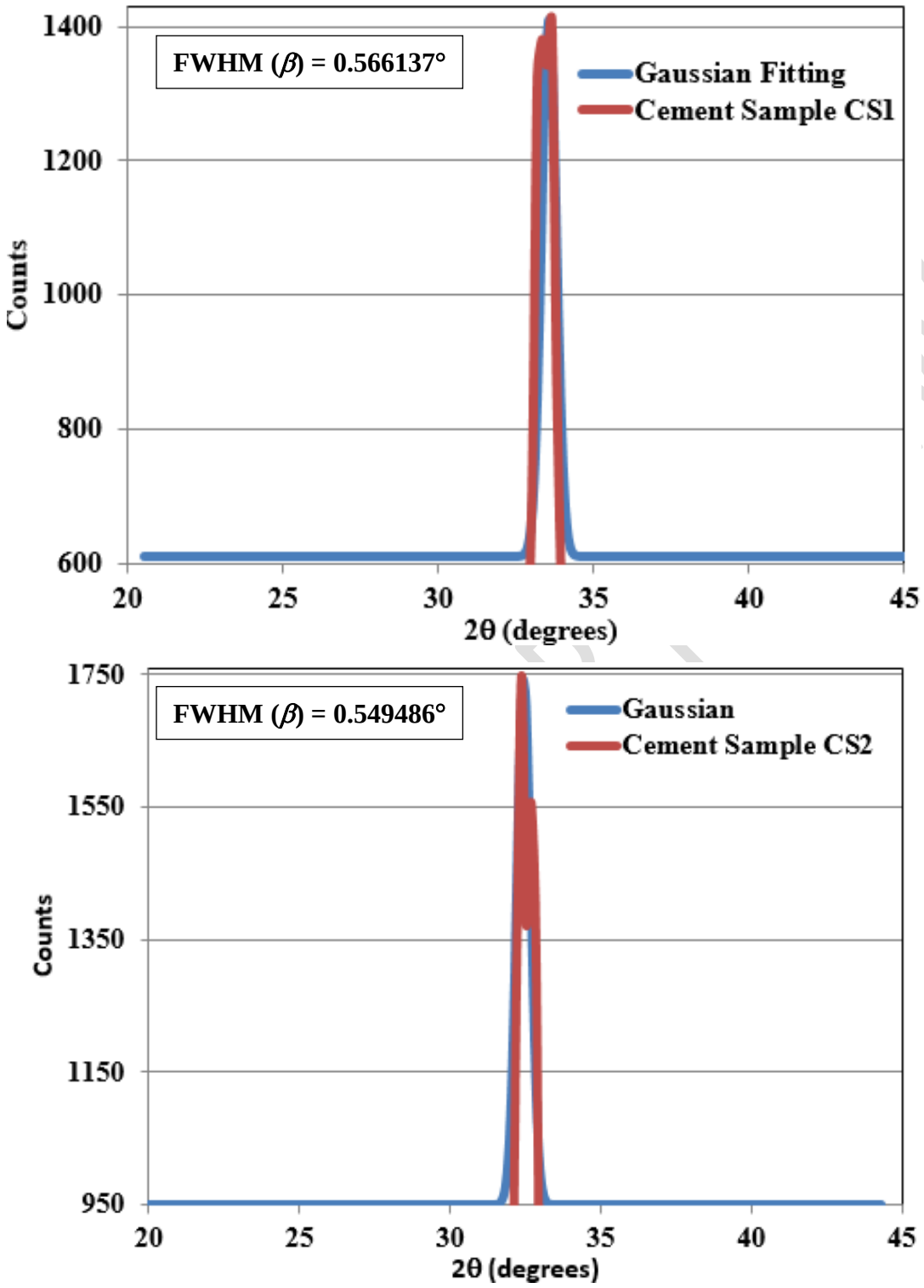

Figure 4. The *Gaussian* convolution fitting of the most intense XRD peak of the cement samples **(A)**CS1 with 2θ = 33.65°, and**(B)**CS2 with 2θ = 32.37°. The concerned FWHM values determined through this peak fitting procedure are mentioned in the

31].The most probable differently sized grains cum particles of each of these sample specimens

speculated from their respective crystallites thickness L are supported quantitatively by the respective number of interatomic parallel planes m stacking in the crystalline materialsdetermined herewith by substituting the concerned values of L and d in Eq. 4. The number of such parallel planes m that are arranged periodically with maintaining gap d in the respective crystallite phases of the respective sample specimens are found to be; m = 58 for CS1, m = 57 for CS2, m = 126 for CS3, and m =119 for CS4 as listed in Table 1. This grain size analyses of the Nepal made cements further underscore herewith the utmostintermixing ratios of each of them with the carbon dust (L = 2 to 12 nm based on the graphitizing temperatures [32]) which is actually not a new technique of the material engineering in the course of stabilizing and enhancing cementitious abilities of the cements. In general, the dosages of carbon dust recommended forenhancing the compressive strength of the cement are in the range of 5% to 40 % by weight of cement [33], and this intermixing proportion is equally suspected to the present cement samples as well. Additionally, the possibility of developing and inventinglow cost supercapacitors and conductive devices by intermixing nano sized carbon powders into the Nepal made cementsamples is also unlocked by these crystallite/grain sizes analyses [34]. Furthermore, all these grain sizes and thickness of the individual sample specimensas a whole illuminate that the cement samples CS1 and CS2 must be handled more safely with adopting particle suppression/dust–free technologies relative to the cement samples CS3 and CS4.The same morphological interpretations provide detailed insights into the particle distributions, fly ash escaping rates, and safety precautions to be assumed by the respective industrial plants and manufacturersfor preventingthe health risks of the industrial workers, site engineers, and all other stakeholders. Thesesize dependency consequences of the cement particles areeventually very helpful to the industry owners for updating their manufacturing policies, workers' guidelines,

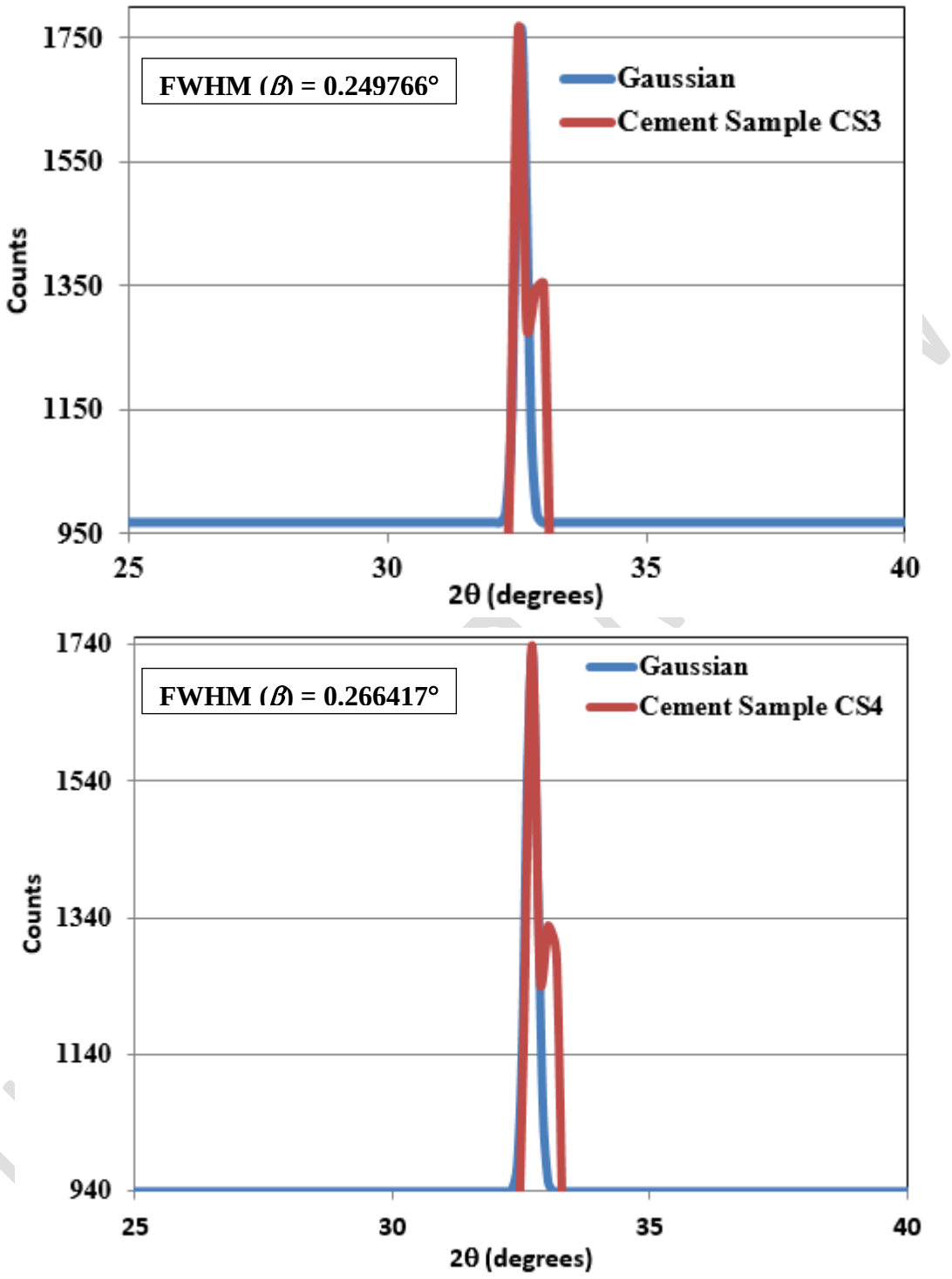

Figure 5. The *Gaussian* convolution fitting of the most intense XRD peak of the cement samples **(A)**CS3 with 2θ = 32.53°, and**(B)**CS4 with 2θ = 32.69°. The concerned FWHM values determined through this peak fitting procedure are mentioned in the

safety precautions, and recruiting strategies. More importantly, this information provides enough

clues towards recommending and acquiring the suitable face masks, face shields, eyes & skin protectors, etc. industrially that are actually designed with the variable pore diameters based on their industrial demands. As a whole, in the viewsof all these potential credentials and most possible hazardous effects, the industrial plants producing CS1 and CS2cements must adopt more severe technologies and safety policies than that of the CS3 and CS4, and make their production workers and site Engineers constraints on them prior to operate the machinery systems in full fledges.The present authors are neither aware of the manufacturing policies and workers' guidelines that are in practice currently in the operating industrial plants of the respective cements in the course of their large scale productions nor the relevant databases are available in their websites, the more criticisms would be impracticable simply on the basis of grain size analyses.

The XRD predicted quantitative crystallite sizes L&grain cum particle sizes plus their specific morphological shapes of the cement samples are also closely associated with the macroscopic observables such as weight (W) and density (ρ). The Nepal made cement samples we analyzed herewith are already known with their maximum percentage fly ash particles with round shapes [5, 18]. Therefore, the present cement specimens CS1, CS2, CS3, and CS4 must have of course excellent packing characteristics but in the different magnitudes. Normally, the greater the range of sizes of the particles cum grains with spherical shapes, the higher is the density of the material. And, the density itself is inversely proportional to the void volume $V_v$of the materials existingin the entire packing structures which in turn relates with their porosity index closely [19, 34]. Based on this principle, the present sample specimens CS1 with L =15.30 nm and CS2 with L =15.71 nm must have the lower densityρ and higher void volume $V_v$plus higher porosity index ηthan thesamples CS3 with L =34.58 nmand CS4 with$L$ =32.44 nm. More

precisely, these XRD predicted crystallite sizes*L*indicate that the first two sample specimens must have almost identical weight*W* and densityρ, and the latter two specimens have in the order W(CS3), ρ(CS3) >W(CS4), ρ(CS4). Moreover, the rates at which the cements absorb water or the specific hydration rates of them are alsodirectly dependent with the grain cum particle sizes,and their specific surface areas as theiroutside layers always act as the host for bearing hydration productswhen the particular cement samples are exposed to the water or high humidity weather scenarios, and as soon as the outer layers of them become fully saturated and extensively thicker, the hydration rates becomesignificantly slower. Additionally, the closed packing plus the closeness of the grains arranged in the cement and cement basedmaterial phasesdetermine the compressive strength and water absorbing propensities or the water/cement ratio [36] of the cements.So, in principle, the smaller is the grain size or the particle size of the cement, the faster will be the reaction ratesor intermixing rateswith water; and the faster will be the kinetics of forming hydration products around the surface of the specific grains/particles. It further means whenever the specific surface area of the grains/particles is larger, more free sites onthem are available to react with the water and to undergo substantial intermixing. Therefore, the present cement samples CS1, CS2, CS3, and CS4 we characterized herewith must show variable water absorbing rates or propensities when exposed fully to the water or to the humid weather conditions though their hydration rates vary with the water exposure timescales in considerable ranges. The sample CS1 with L =15.30 nm and CS2 with L =15.71 nmmust exhibit a speedychemical kinetics associated with the reaction rates between the cement particles and water than that of the samples CS3 with L=34.58 nmand CS4with$L$ =32.44 nm.More explicitly, the reaction rates of them with the water (hydration rates) would be in the order of CS1>CS2>CS4>CS3. This granular size dependent chemical kinetics of the hydration reactions

of each cement sample specimenscan be materializedgenuinely if one can further probe the quantity of the hydration products deposited around the spherical particles of the cements as a function of hydration timewith precise experimental techniques. The present authors are currently unable to express the same in quantitative scales as this work was carried out mainly to characterizethe cement materials ratherto present their hydration rates and to identify the distinguishable hydrated products.

In cement and cement based materials, the grain sizes cum particle sizes *L*act as the most decisive parameters for understanding their plastering/adhering/cementing/setting propensities. In principle, the most critical descriptors that control the concerned cementation/hardening/setting/gaining strength, etc. rates of the cements are their particles sizes and the thorough distributions of them in the cement pastes [37].If the sufficient amount of small particles exist in the cements, their hydration and setting rates would be much quicker with good adhering and compressive strengths. And, contrastingly,if the cements are made up of predominantly with the too many smaller particles, they undergo immediate setting but possessing poor intermixing and placing abilities. Therefore, the cements with good particle size distributionsare always designated as high standard, and are preferable for designing engineering structures and strengthening their foundations. According to the literature analyses, the complete hydration and setting times for the cements that contain the predominant particles with a diameter of1μm, and 10μm are one day, and one month respectively, butthat for the cements with the particles of diameter 50μm never reachesto the fully hydrated stages even exposed to water sufficiently [38, 39]. Even though the thorough particle sizes distribution analyses of the present cement sample specimens CS1, CS2, CS3, and CS4 are not carried out here, and are not made available publicly by their respective manufacturers, being the cement samples CS1

(L =15.30 nm) and CS2(L =15.71 nm)comprising with the comparable grain cum particle sizes, they are claimed here to exhibit good yet almost identical setting time along with showingextraordinary intermixing efficiencies with water relative to thosewith the CS3 (L = 34.58 nm) and CS4 (L = 32.44 nm) samples.In particular, the cementation and setting rates of them can be speculated here in the order; CS1 > CS2 > CS4> CS3 though it is subjected to change slightly if they are probed with the sophisticated particle size analyzers, and inquiredtheir in-depth particle sizes distributions closely. Despite having all these consequences and the most probable yet variable adhering/cementation rates of the four different sample specimens analyzed herewith, theyall are good enough toattain preferable strengths&reasonable dryings in a shorter time, and to have less risks of cracking due totheir in-built compositionsas OPC types (the OPC type cements always harden quicker than the Pozzolonic Portland Cement (PPC) type) [40]. However, they are relatively more suffered from the heat releases of ~60°C during hydration reactions, and the need of excessive caring and curing in a lesser extent of time (post-treatment/post-curing attentions).All these significant applicative physicochemical properties of the cements are further due to the presence of variable percentage compositions of the chemical constituents and functional groupsanalyzedin the subsection 3.2.

3.2 Interpretations of the FTIR Spectrograms

Alike to the XRD instrumentation technique and its remarkable performance of analyzing the solid state powdered samples in quantitative scales,the Fourier Transform Infrared (FTIR) spectroscopy is also one of the most potential and trustworthy instrumental methods that enables the chemists to investigate the cementitious chemical constituents present in the OPC type cements quantitatively. Being the cements and cement based materials comprising with the various types of the chemical constituents holding unique functional groups, such as Si–O,

SiO_4^{4-}, SO_4^{2-}, OH^-, Al–O, CO_3^{2-}, Al_2O_3 (Alumina), MgO (Magnesia), SO_3, etc., and the FTIR

technique bestowing the skills of tracing all the infrared active vibration modes of each of the

chemical bonds of all these wide rangedchemical components explicitly, the extensive

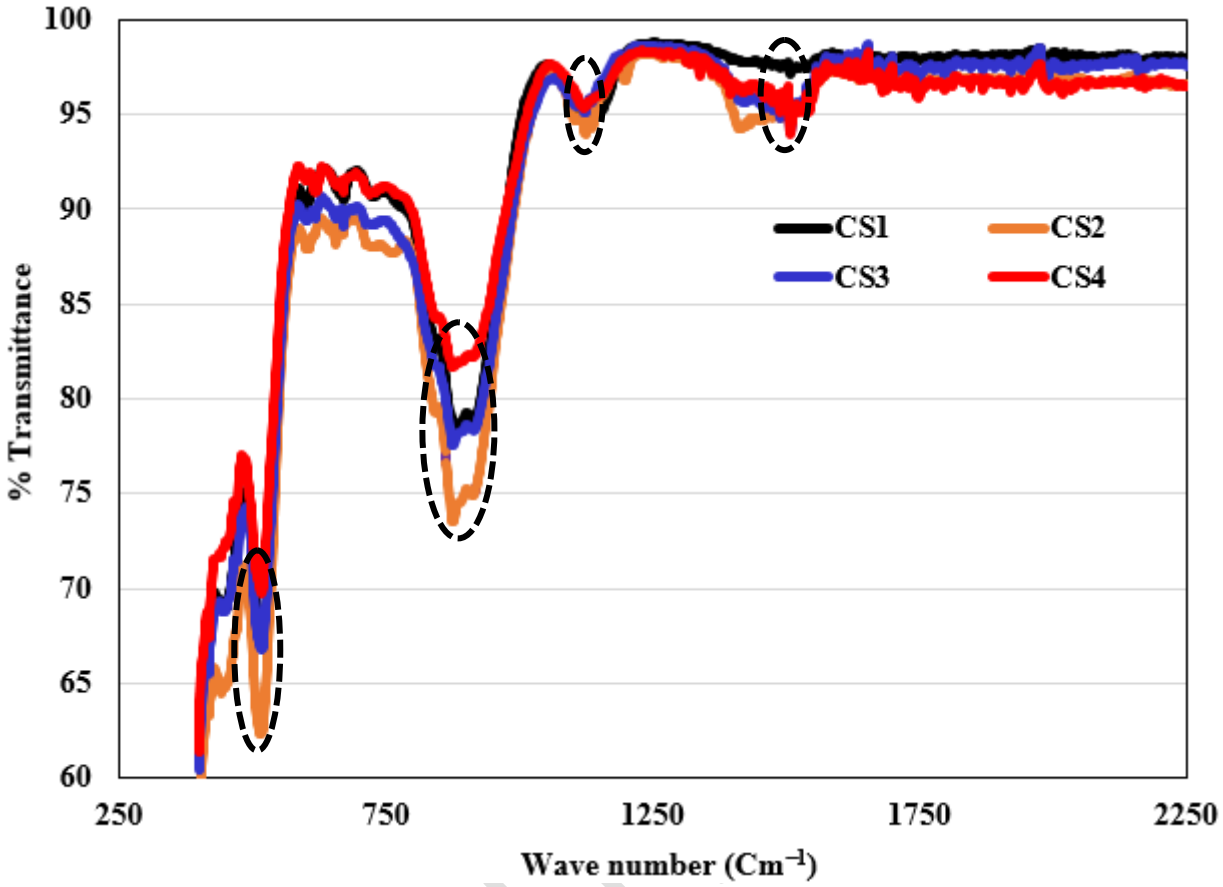

Figure 6. The IR spectra of the cement samples CS1, CS2, CS3, and CS4 measured with the Shimadzu IR Affinity–1S (S.No.AZ1965904022) spectrometer. The most intense IR peaks of all the samples appeared at wave numbers ~515 cm^{-1}, ~900cm^{-1}, 1125cm^{-1}, and 1500$cm^{-1}$are encircled by the oval shapes. The respective spectral regions are zoomed out in Figure 7 and Figure 8 for making the spectral lines magnificent and the related spectral interpretations easier.

employment of this instrumentation tool and its precise application features in characterizing the

plain and hydrated cements and cement based materials is not new in material engineering [5, 9,

24, 25, 41–43]. Additionally, based on the raw materials used in manufacturing cements such as

limestone/chalk ($CaCO_3$), silica (SiO_2) and alumina (Al_2O_3) of clay and shale, etc. and their

explicit internal chemical compositions plus their combined matrix or modulus forms developed

in the course of preparing the clinker balls, the direct employment of the FTIR tools in

identifyingall the fundamental chemical constituents and their functional groupsis recognized as

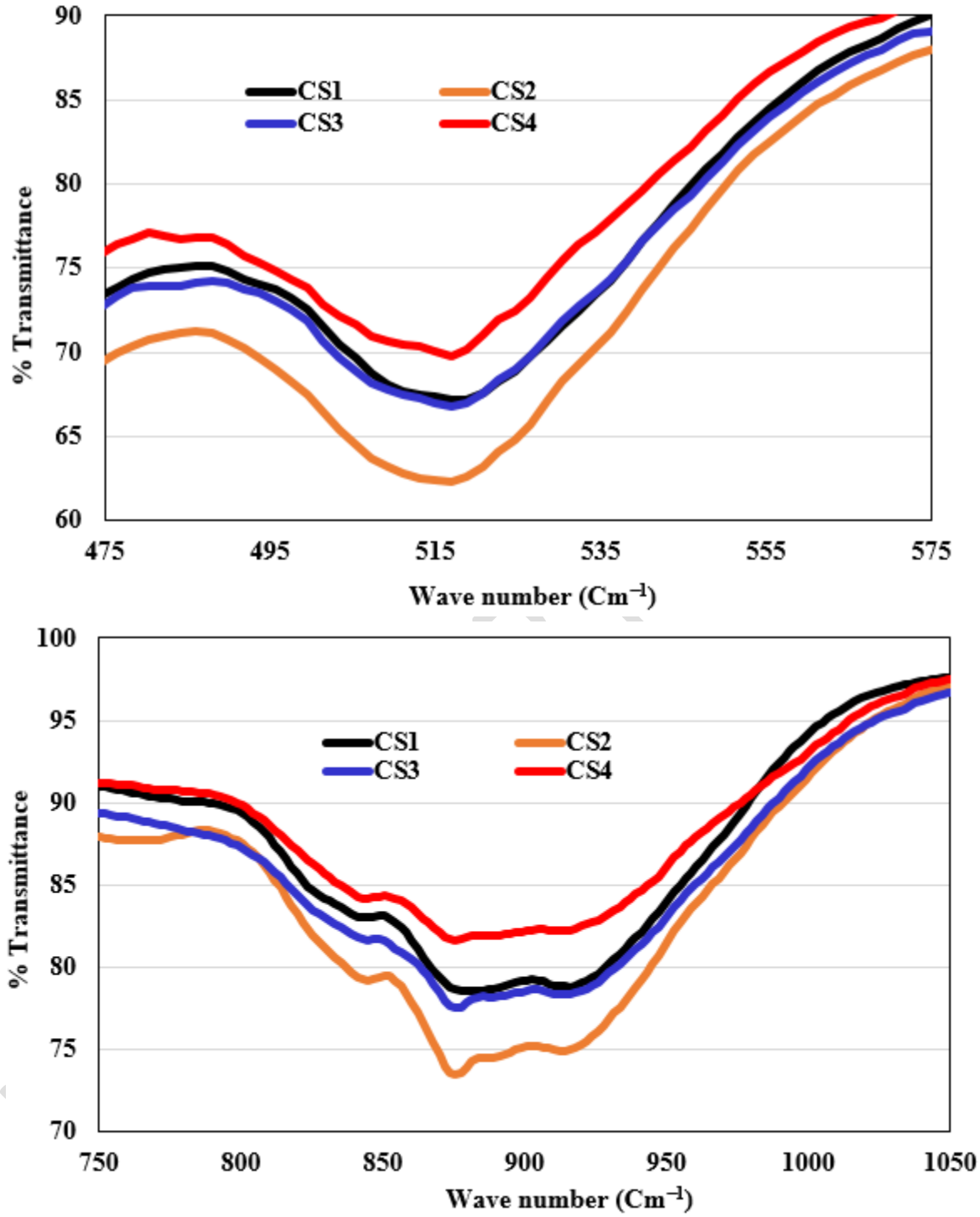

Figure 7. The zoomed outIR spectra of the cement samples CS1, CS2, CS3, and CS4 at the regions of the first two IR peaks appeared at wave numbers **(A)**~515 cm^{-1}, and **(B)**~900cm^{-1} as encircled in Figure 6.

an indispensable mean which in fact makes this facility one of the most standalone applications.

The present study utilizes the same applicative features of the FTIR, and characterizes the four different OPC cement samples CS1, CS2, CS3, and CS4 available in the commercial markets of Nepal in respect to the IR active vibration modes of the specific chemical bonds of their primarychemical constituents, and the associated functional groups plus their peak shifting due to surrounding chemical groups/fragments. The concerned FTIR spectrogram of the four different sample specimensis shown in Figure 6 where the most intense IRpeaks appeared at the wave numbers ~515 cm^{-1}, ~900 cm^{-1}, 1125 cm^{-1},and 1500 $cm^{-1}$are encircled. The respective spectral regions aremagnified in Figure 7 and Figure 8 for visualizingall the spectral lines and for easing therelated spectral interpretations explicitly. All the sharp intense and diffuse IR bands are identified by referring the standard databases available in different scientific literatures [5,42,44–50]. The first IR active region at ~515 $cm^{-1}$of each of the cement samples is the designated position for the out-of-plane Si–O bending, the second intense IR peak at 870 $cm^{-1}$is typical for amorphous calcium carbonate (hereafter, ACC) and the peak at 876 cm^{-1} is assigned to CO_3^{2-}, and the third intense IR active peak appeared at 920$cm^{-1}$is due to the asymmetric Si–O stretching vibrations of the dicalcium silicate ($2CaO.SiO_2$) and tricalcium silicate ($3CaO.SiO_2$) type chemical compounds; the most abundant type chemical compounds present in the current OPC type cements [42–45]. In fact, these characteristic vibrations are arisen from the atomic motions within the silicate (SiO_4^{2-}) tetrahedra. The absolute presence of the SiO_4^{2-} units and the SiO_4^{2-} holding chemical compounds in the present cement samples is also guaranteed by the IR bands appeared in the regions between ~660 cm^{-1} – ~670 cm^{-1}, and ~440 cm^{-1} – ~450 cm^{-1} [42, 46]. The broad IR peaks of each sample specimen seen in the regions of ~615 cm^{-1} (Al–O; Al–OH vibration modes) exemplify the presence of hardening chemical constituentsalumina (Al_2O_3) and Al_2O_3 based chemical compounds in trace amounts. It meets the criteria of industrial

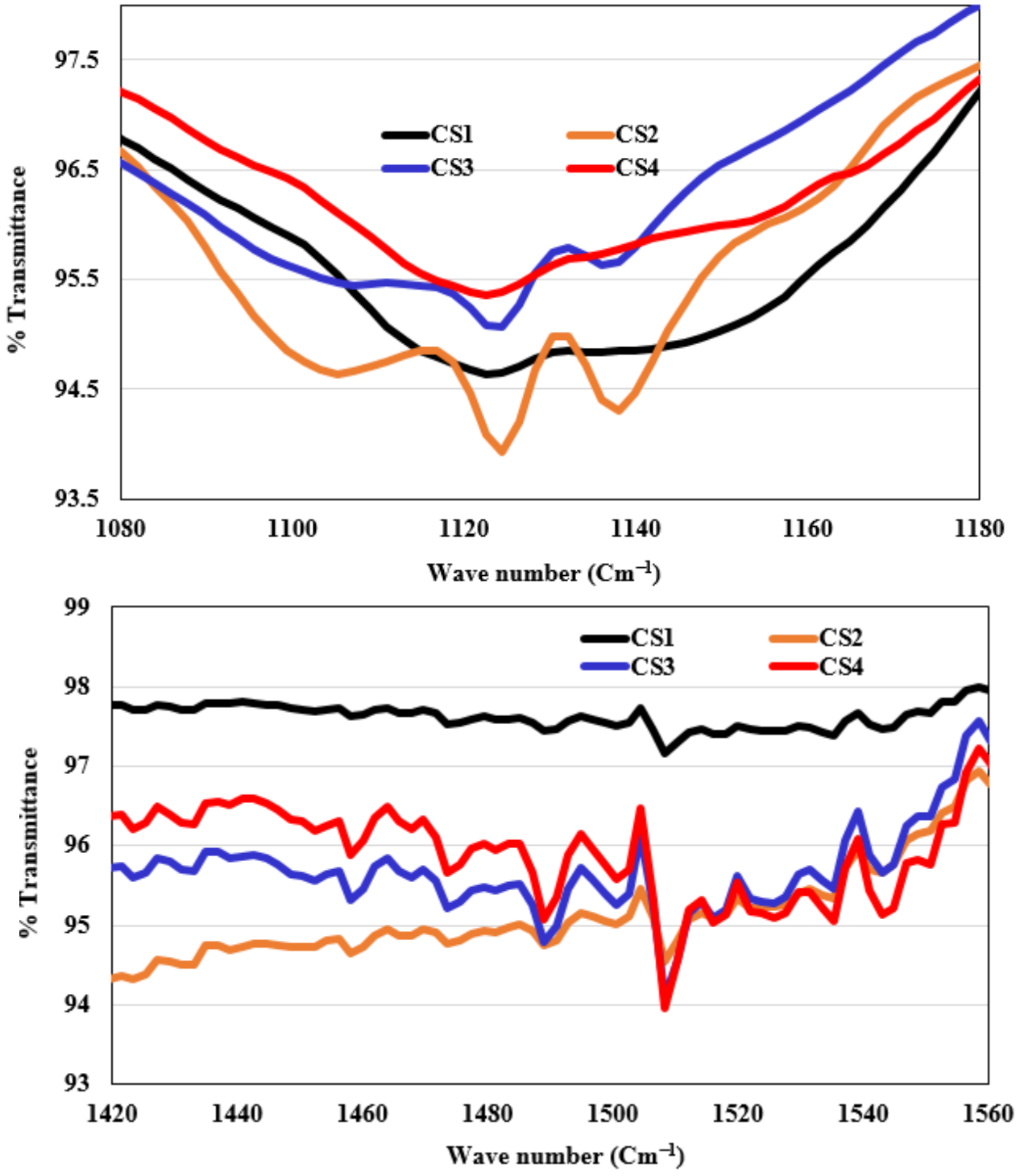

Figure 8. The zoomed outIR spectra of the cement samples CS1, CS2, CS3, and CS4 at the regions of the last two IR peaks appeared at wave numbers**(A)** ~1125 cm^{-1}, and**(B)** ~1500cm^{-1} as encircled in Figure 6.

needs: all the OPC type cements are industrially manufactured by maintaining significantly less

(more)percentage composition of the Al_2O_3 basedquick binder unlike to that of the aluminous cement (PPC cement) [49].However, no IR bands are appeared at all in the low wavenumber regions including 554 cm^{-1}, and 465 cm^{-1}, attributing to the complete absence of pseudoboehmite ($AlOOH.xH_2O$) type aluminum compounds in every cement samples [50], and the complete absence of IR band in 548 cm^{-1}(the typical IR band for Mg–O stretching mode) [51] confirms that no magnesia (MgO) and MgO based chemical compounds are present in each of them. The fourth intense peak appeared at the region of~1120cm^{-1}– ~1140 cm^{-1} is due to the presence of divalent SO_4^{2-}radicals(gypsum ($CaSO_4 \cdot 2H_2O$)) in the cement samples [5]. The absolute absence of the IR peak at 855 cm^{-1} confirms that no heavy $CaCO_3$ with high content of aragonite (a carbonate mineral formed by the biological and physical processes) is present in all the four cement samples whereas the typical presence of the IR band at 873 cm^{-1} suggests that each of them predominantly contains the light $CaCO_3$ with high percentage of calcite phases.Additionally, the complete absence of IR active vibration modes in the region ~2800 cm^{-1} – ~2900 cm^{-1} assures that none of the cement samples contain active $CaCO_3$ with the traces of the organic compounds [45, 46]. Again, the splitting IR band appeared at ~1420 cm^{-1} indicates the presence of typical type ACC, and the sharp IR peaks appeared at ~720 cm^{-1} and ~ 877 cm^{-1}further underscores the completepresence of the calcite phases (light $CaCO_3$) in all the four cement samples.The similar presence of $CaCO_3$asthe major chemical constituents in all the four different cement samples is also confirmed by the typical CO_3^{2-}peak appeared at the region of ~1520 cm^{-1}.Additionally, the diffused type IR peaks of all the four different cement samples appeared at the regions of ~620 cm^{-1}signify that the trace amount of the pentavalent arsenic As^{5+}–bearing oxyanions (AsO_4^{3-}) containing chemical compounds $CaHAsO_4.2H_2O$, $CaH_4(AsO_4)_2.2H_2O$, and $Ca_3(AsO_4)_2$[24] are present in them as predicted from the XRD derived

interlayer distance d values (subsection 3.1).Theseinterpretations reveal that all the four different cement samples are mostly comprising with the almost same type of the chemical constituents. However, the appearance of relatively low height and diffused type peaks at the region of ~1180 cm^{-1}(typical position for symmetric SO_3^{2-} stretching) for the samplesCS1, CS2, and CS3indicates that no CS4 cement sample contains SO_3^{2-} and SO_3^{2-} based chemical compounds at all. The closed inspection of the spectrogramfurther verifies that there is a complete absence of the IR active bandsin the regions of~3100 cm^{-1}– ~3400 cm^{-1} (this region is excluded on the x–axis of Figure 6);the typical position forthe O−H stretching vibration modesof the H_2O molecules. It ensures that none of the cement samples we submitted for the instrumental analyses adsorb significant levels of the humidity. Furthermore, while comparing the spectral IR bands of the hydrated OPC cement specimens to that of the dry cement samples inspected herewith, all the significant IR active bands appeared in the regions ~720 cm^{-1},~900 cm^{-1}, 1125 cm^{-1},and 1500 cm^{-1} are found to be reproduced well [47]; indicating that every cement samples(CS1, CS2, CS3 and CS4) retaintheircalcite phases, silicate (SiO_4^{4-}) phases,dicalcium silicate ($2CaO.SiO_2$)&tricalcium silicate ($3CaO.SiO_2$) compounds, and the chemical components holding CO_3^{2-} unitwhile undergoing complete hydration reactions (reaction with water) for the specific timeperiod. This retentiveness ability of the cement is very much needful yet applicative to inspect the placing and hardening propensities of the cements and their hydrated pastes. All these specific IR active bands of the present cement samples are even found to be unshiftedat all to that of the similar type OPC cements mixed thoroughly with the 0.07% of graphene oxide and reduced graphene oxide powders separately for 7 days [47]; further ensuring that the oxygen-containing functional groups (=O, –OH, –O–, –COOH) of the carbon materialcan be mixed thoroughly to the Nepal made cement samples in order to enhance theircementitious abilities.

This specific material based characteristic features needs more quantitative justifications and investigations for further materializing them in the Nepal made cement brands. The present authors limit the related interpretations this much due to the shortage of enough literature basedfacts.

Even though the fundamental chemical constituents and the related chemical compounds present in each cement sample specimens inspected in this study are predicted as almost same, the quantitative proportions of them are unique in each brand as the intensity of the concerned IR bands, their depth, their total specific peak area, and their peak broadening are appeared as contrastingly different.Herewith, present authors have neither estimated the specific peak area of each intense IR band nor determined the number density of the functional groups and the chemical components quantitatively as it lies beyond the principal objectives of this research work.But, some qualitative informationretrievedherewith just by inspecting the specific IR bands of each sample specimens, and by comparing their intensity depth, and specific peak area obviously provides in-depth knowledge of the chemical constituents and their percentage compositions. As shown in Figure 7 and Figure 8, each of the four cement samples has unique depth and intensity of the specific IR bands appeared in the regions of ~515 cm^{-1}, ~900 cm^{-1}, 1125 cm^{-1},and 1500 cm^{-1}; signifying the utmost possibility of consisting ofdissimilar proportions of the chemical constituents. More explicitly, the quantitative proportions of the dicalcium silicate ($2CaO.SiO_2$), tricalcium silicate ($3CaO.SiO_2$) type chemical compounds and the SiO_4^{2-} tetrahedra bearing chemical components present in the cement samples are found in the trend of CS2 > CS3 >CS1 > CS4, as their IR bands at ~515 cm^{-1}in Figure 7(A) show the respective depth intensity (peak area) in the same trend. The explicit IR bands with different depth intensity at ~900 cm^{-1}(Figure 7(B)) assigned mostly tothe calcium carbonate, and calcite

phases further predict their dissimilar quantitative proportions in the cement samples as CS2 > CS3 > CS1 > CS4. Similarly, the individual IR bandsat the region of ~1125 cm^{-1} assigned to the divalent SO_4^{2-} radicalsand the SO_4^{2-} based chemical components, and their particular depth intensity (Figure 8(A))approximately depict their quantitative amounts in the trend CS2>CS3.These type of the chemical constituents are relatively less in quantity and show their presencein trace amountsin the samples CS1 and CS4 (both have very broad and diffused type peaks). Moreover, the typical CO_3^{2-}peaks appeared at the region of ~1500 cm^{-1}(Figure 8(B)) and their specific peak area reveal the quantitative proportions of the CO_3^{2-} bearing chemical constituents in the trend CS4 > CS3 > CS2 > CS1, and almost equally intense IR bands at the regions of ~620 cm^{-1}attributing to the pentavalent arsenic As^{5+}–bearing oxyanions (AsO_4^{3-}) containing chemical compounds[$CaHAsO_4.2H_2O$, $CaH_4(AsO_4)_2.2H_2O$, and $Ca_3(AsO_4)_2$] signify their identicalpercentage in all the sample specimens. Even though the explicit roles of these chemical constituents in the Nepal made cement samples lie under further investigations, thespecific quantitative predictions of them made herewith eventually provide the indispensable guidelines to the industrial sectorsfor the sake ofinnovating more branded cements and of improvising their workability plus advancing their cementitious abilities. Thuspresented results are ultimately very useful to boost up the production rates of the industrial plants and to meet the standard norms of the cements aligned to fulfill the public demand rates of the latter in the commercial markets.

4. CONCLUSIONS

This research work was basically aimed at characterizing the different brand cements available in the commercial market of Nepal that are in peak demands due to their good qualities and exceptional performances in engineering and construction sectors. While the Nepalese

annual per capita cement consumption rate is 303kg, and is already speculated nationwide as 26million tons/year by the end of the fiscal year 2024–2025, and the various national mega construction projects with rapid urbanization pace are periodically in progress across the country that further surge the national demands of good quality cements day to day, the foreign installed, state–owned, and the privately financed cement industries rarely offer a large scale research opportunities and instrumental characterization facilities, allocate enough R & D budgets, provide research internships, and extend innovation & designation platforms intensively. On the one hand, the existing cement industries in Nepal are facing several challenges out of which the timely non-disruptive supply of the good grades clinker from the foreign lands andthe shortage of the skilled workforce designated for the specific R & Dpurposes are the major ones, but on the other hand, they are constantly looking for the continuous industrial pace of the development, advancement, improvement, and innovations of the esteemed cements productsso that they can fulfill the public consumption ratesand demands of the latter in the commercial markets. These sorts of industry-academia gaps can be minimized collectively by characterizing the regularly supplied clinker based ingredients, closely associatedraw materials, and the ready-to-use dry cements themselves,installing the latest yet sophisticated cement manufacturing technologies, and implementing the benchmark manufacturing and products distributing policies. In this arena, the present state-of-art X–ray diffraction (XRD) and Fourier Transform Infrared (FTIR) spectroscopy basedinstrumental characterization studiesof the variable manufactured ready-to-use dry cement samples named explicitly herewith as CS1, CS2, CS3, and CS4are believed to add substantial values.

As per the XRD derived most intense spectral peak of each of the cement samples at 2θ = ~ 33°, all of them were found to contain significant levels of $CaCO_3$ phases. The smallest

interlayer distance d (CS1) = 2.7Å derived from the same technique suggestedthat cement CS1 has the most closely packed interatomic layers crystalline phases, and the almost identical value of d (d = 2.8Å) for the rest of the cement samples confirmed their crystalline phases comprising with the comparable interlayer packing ratios. The aggregable range of these d values to that of the As^{5+}–bearing oxyanions (AsO_4^{3-}) Portland cement type–V (d= 2.8Å to 3.0 Å) exemplified that each of the cement samples contain the phases of $Ca(OH)_2$ (d = 2.7Å), $CaCO_3$ (d = 2.9Å),$CaHAsO_4.2H_2O$ (d = 2.9Å), $CaH_4(AsO_4)_2.2H_2O$ (d = 2.2Å) and $Ca_3(AsO_4)_2$ (d = 2.9Å) type chemical compounds as their stabilization/solidification (S/S)matrix constituents. The estimated value of the crystallite size Lofthe samples CS1 (L =15.30 nm) &CS2 (L =15.71 nm), and CS3 (L=34.58 nm) & CS4 (L=32.44 nm) were found to be as equal as that measured for the $MnFe_2O_4$ spinel nanoparticles based OPC cement (L = 16 nm) and the calcite based OPC cement (L=30 nm) respectively.Almost half in Lvalue of the former two cement samples described that their crystallites grow and agglomerate each other by producing relatively smaller particle or grain sizes than that of the latter two samples, and equally underscored their utmost intermixing ratios with the carbon dust (L = 2 nm–12 nm); eventually signified the maximum chances of stabilizing and enhancing cementitious abilities of the Nepal made cements, and unlocked the possibility of developing/inventing low cost supercapacitors and conductive devices simply by mixing the cement with carbon genuinely. Based on the same L values, the former two samples were predicted to have the lower density ρ and higher void volume $V_v$plus higher porosity index ηthan the lattertwo samples. The same analyses speculated the distinguishablehydration rates of them when exposed fully to the water, and hence is the variable setting time plus intermixing efficiencies with water in the trendCS1> CS2 > CS4 >CS3. Similarly, the most intense IRpeaks appeared in the regions ~515 cm^{-1}, ~900 cm^{-1},920 cm^{-1},and 1125 $cm^{-1}$of the FTIR spectrogram

of each of the cement samples confirmed their silicate (SiO_4^{2-}) tetrahedra based chemical components, amorphous calcium carbonate phases and the CO_3^{2-} unit holding chemical constituents, dicalcium silicate ($2CaO.SiO_2$) and tricalcium silicate ($3CaO.SiO_2$) type chemical compounds respectively. The absolute presence of the SiO_4^{2-}units and the SiO_4^{2-} holding chemical compounds in them wasalso guaranteed by the IR bands appeared in the regions between ~660 cm^{-1} – ~670 cm^{-1}, and ~440 cm^{-1} – ~450 cm^{-1}. The presence of trace amounts of hardening chemical constituent alumina (Al_2O_3), and Al_2O_3 based chemical compounds in each of them was assured by the broad IR peaks seen in the regions of ~615 cm^{-1}, but the complete absence of pseudoboehmite ($AlOOH.xH_2O$) and magnesia (MgO) based chemical compounds in them was revealed by the disappearance of the IR bands specifically in the low wavenumber regions (~554 cm^{-1}, ~465 cm^{-1}, and ~548 cm^{-1}). Again,neither the presence of heavy $CaCO_3$ with high content of aragonite nor the active $CaCO_3$ with the traces of organic compounds in them was made sure by the absolute absence of the IR peak at ~855 cm^{-1}, and ~2800 cm^{-1} – ~2900 cm^{-1}, instead the predominant content of the light $CaCO_3$ with high percentage of calcite phases in them was disclosed by the typical IR band appeared at 873 cm^{-1}.Additionally, the XRD suspectedtrace amounts of the pentavalent arsenic As^{5+}–bearing oxyanions (AsO_4^{3-}) containing chemical compounds ($CaHAsO_4.2H_2O$, $CaH_4(AsO_4)_2.2H_2O$, and $Ca_3(AsO_4)_2$) in each cement samples were confirmed by the diffused type IR peaks appeared at ~620 cm^{-1}. Moreover, the quantitative proportions of the dicalcium silicate ($2CaO.SiO_2$), tricalcium silicate ($3CaO.SiO_2$), SiO_4^{2-} tetrahedra bearing chemical components, calcium carbonate, and calcite phases present in each cement sampleswereapproximated by analyzing the peak area, and the concerned depth intensity of the designated IR bands, and were found as CS2 > CS3 >CS1 > CS4. In contrast to this, the quantitative proportions of the CO_3^{2-}groups bearing chemical constituents were

estimated in the trend CS4 > CS3 > CS2 > CS1, and that of the AsO_4^{3-} holding chemical compounds in them was speculated as almost identical.

As a whole, all these characterizations made through the sophisticated instrumentation techniques would be highly useful to standardize the industrial cement manufacturing guidelines of Nepal, to improvise the quality of Nepal made cements, and to expedite their working, adhering, placing, and cementitious abilities.Towards these potential prospective, this article stands as a doctrine document not only for regulating the constant demands/supplies of the standard yet good grade cements, acquiring the consistent quality control & dependable cement and cement based products nationwide, but also for assessing the industrial health, safety, and accidental prevention schemes specifically.

REFERENCES

1. Govindarajan D, Gopalakrishnan R. Spectroscopic studies on Indian Portland cement hydrated with distilled water and sea water. Frontiers in Science. 2011; 1:21–27.
2. Mehta PK, Monteiro PJ. Concrete: Microstructure, Properties, and Materials. McGraw-Hill Education; 2013.
3. Mindess S, Young JF, Darwin D. Concrete. Prentice-Hall, Upper Saddle River; 2003.
4. Kosmatka SH, Kerkhoff B, Panarese WC. Design and Control of Concrete Mixtures. Portland Cement Association, 5420 Old Orchard Road Skokie, Illinois; 2008.
5. Shrestha SL. Characterization of Some Cement Samples of Nepal Using FTIR Spectroscopy. International Journal of Advanced Research in Chemical Science. 2018; 5 (7):19–23.
6. Neville AM. Properties of Concrete. Pearson Education; 2011.
7. Kumar R. Nepal struggles to balance nature and industry. Nepali Times. 2022

8. Available: https://nepalitimes.com/banner/nepal-struggles-to-balance-nature-and-industry

9. (a) Prasain K. Nepal will require 26 million tonnes of cement annually by 2024-25. The Kathmandu Post. 2021

10. Available: https://kathmandupost.com/money/2021/05/21/nepal-will-require-26-million-tonnes-of-cement-annually-by-2024-25-report-says#:~:text=Krishana%20Prasain&text=Nepal%20is%20estimated%20to%20require,Rastra%20Bank%20on%20Friday%20showed.

11. Nepal become self-reliant in clinker. Khabarhub. 2019

12. Available: https://english.khabarhub.com/2019/09/53872/

13. Pandey PR, Banskota N. Process of cement production in Nepal. Bulletin of the Department of Geology, Tribhuvan University. 2000; 11:71–78

14. Cement in Nepal. 2020

Available: https://oec.world/en/profile/bilateral-product/cement/reporter/npl

15. Nepal cement worth 170 million exported. NepalNews: Rastrita Samachar Samiti. 2023

Available: https://nepalnews.com/s/business/nepal-cement-worth-170-million-exported#:~:text=Two%20Nepali%20cement%20industries%20have,cement%20since%20October%2017%2C%202022.

16. Nepal Academy of Science and Technology (NAST): Science & Technology for National Development. 2023.

Available: https://nast.gov.np/

17. Research instrumentation standard operating procedure for bruker d2 phaser powder x-ray diffractometer (oppxrd-1) at NUCS FULMER. Revision 0.0. 2012.

Available:https://s3.wp.wsu.edu/uploads/sites/2909/2022/06/OPPXRD-1-Operating-Procedure -for-Powder-X-ray-Diffractometer-Rev.-03-2022.pdf

18. Research Center for Applied Science and Technology. 2023. Available: https://recast.edu.np/

19. Shimadzu Corporation. Instruction manual user system guide IR affinity-1 Shimadzu Fourier transform infrared spectrophotometer Available: https://centrallab.ubonab.ac.ir/uploads/user/161/image/equipments/chempolyengineering/catalogs/shimadzu%20userguide_affinity.pdf

20. Mukhopadhyay A, Ganesh RM, Liu KW, Deng Y. Direct determination of cement composition by X-ray diffraction. Technical Report 0-6941-R1. 2019. Available:https://static.tti.tamu.edu/tti.tamu.edu/documents/0-6941-R1.pdf

21. Ali A, Chiang YW, Santos RM. X-ray Diffraction Techniques for Mineral Characterization: A Review for Engineers of the Fundamentals, Applications, and Research Directions. Minerals. 2022; *12*(2):205(1–25).

22. Tao Y, Gautam BP, Pradhan PM, Hu C. Characterization and reactivity of Nepali clays as supplementary cementitious material. Case Studies in Construction Materials. 2022; 16: e00947(1–12).

23. Ma J, Wang D, Zhao S, Duan P, Yang S. Influence of Particle Morphology of Ground Fly Ash on the Fluidity and Strength of Cement Paste. Materials. 2021; 14, 283:2–18.

24. Langford JI, Wilson JC. Seherrer after Sixty Years: A Survey and Some New Results in the Determination of crystallite size. Journal of Applied Crystallography.1978; 11: 102–113.

25. Smilgies DM.Scherrer grain-size analysis adapted to grazing-incidence scattering with area detectors. Journal of Applied Crystallography. 2009; 42:1030–1034.

26. Mukhopadhyay A, Ganesh RM, Liu KW, Deng Y. Direct Determination of Cement Composition by X-ray Diffraction. 2019; 1–89.

27. Chauhan A. Usage of Powder XRD Technique for Material Characterization and Analysis of Portland cement. Journal of Analytical and Bioanalytical techniques. 2015; 6:e123.

28. Mollah MYA, Kesmez M, Cocke DL. An X-ray diffraction (XRD) and Fourier transform infrared spectroscopic (FTIR) investigation of the long-term effect on the solidification/stabilization (S/S) of arsenic (V) in Portland cement type-V. Science of the Total Environment. 2004; 325:255–262.

29. Mollah MYA, Lu F, Cocke DL. An X-ray diffraction (XRD) and Fourier transform infrared spectroscopic (FTIR) characterization of the speciation of arsenic (V) in Portland cement type-V. Science of the Total Environment. 1998; 224:57–68.

30. Cocke DL, Mollah MYA. The chemistry and leaching mechanisms of hazardous substances in cementitious solidification-stabilization systems. Chemistry and microstructure of solidified waste forms. 1993; 187–242.

31. Baxter S. Cement compositions containing nano sized boehmite crystallites. United States Patent Application Publication. Pub. No.: US 2014/0224156A1, 2014 Available:https://patentimages.storage.googleapis.com/2c/77/e1/0d542d709d235f/US201402 24156A1.pdf

32. Mohamed OA, El-dek SI, El-Gamal SMA. Mechanical performance and thermal stability of hardened Portland cement-recycled sludge pastes containing $MnFe_2O_4$ nanoparticles. Scientific Reports. 2023; 13:1–21.

Available: https://www.nature.com/articles/s41598-023-29093-y

33. Lilkov V, Petrov O, Kovacheva D, Rostovsky I, Tzvetanova Y, Petkova V, Petrova N. Carbonation process in cement with mineral additions of natural zeolite and silica fume – Early hydration period (minutes) up to 24 hours. Construction and Building Materials. 2016; 124:838–845.

34. Shiraishi M, Inagaki M. X-ray Diffraction Methods to Study Crystallite Size and Lattice Constants of Carbon Materials. Carbon Alloys. 2003; 161–173.

35. Głuchowski P**,** Tomala R, Kujawa D, Boiko V, Murauskas T, Solarz P. Insights into the Relationship between Crystallite Size, Sintering Pressure, Temperature Sensitivity, and Persistent Luminescence Color of $Gd_{2.97}Pr_{0.03}Ga_3Al_2O_{12}$ Powders and Ceramics. Journal of Physical Chemistry C. 2022;126(16):7127–7142.

36. Unga´r T, Gubicza J, Tichy G, Pantea C, Zerda TW. Size and shape of crystallites and internal stresses in carbon blacks. Composites: Part A: Applied Science and Manufacturing. 2005; 36:431–436.

37. Irshidat MR,Alnuaimi NA. Industrial Waste Utilization of Carbon Dust in Sustainable Cementitious Composites Production. Materials. 2020; 13(15):3295(1–13).

38. Patel P. Mixing carbon nanopowder into cement gives a low-cost supercapacitor. Chemical & Engineering News. 2023;101(26):

39. Guida G, Casini F. Packing density of bi-disperse mixtures under one-dimensional compression. Powders and Grains. 2021; 249:07012.

40. Wang LC. Experimental Study on Water Absorption by Concrete Damaged by Uniaxial Loading. 4th International Conference on the Durability of Concrete Structures. 2014; 24–26.

41. Singh VK. The Science and Technology of Cement and Other Hydraulic Binders. Woodhead Publishing. 2023.

42. Mamlouk M, Zaniewski J. Materials for Civil and Construction Engineers. Addison Wesley Longman, Inc. 1999.

43. Mindess S, Young JF. Concrete. Prentice-Hall, Inc., Englewood.1981.

44. Purushotham Reddy K, Chandra Mohan Rao BDV, Maganti JM, Swamy Naga Ratna GP. Comparative studies on LC_3 based concrete with OPC & PPC based concretes. Materials Today Proceedings. 2021; 43(2):2368–2372.

45. Ghosh SN, Handoo SK. Infrared and Raman spectral studies in cement and concrete. Cement and Concrete Research. 1980;10:771–782.

46. Mollah MYA, Parga JR, Cocke DL. An infrared spectroscopic examination of cement based solidification stabilization systems-Portland type-V and type-IP. Journal of Environmental Science Health. 1992; 27:1503.

47. Mishra AK, Jha A. Quality Assessment of Sarbottam Cement of Nepal. International Journal of Operations Management and Services. 2019; 9(1):1–22.

48. Cai GB, Chen SF, Liu L, Jiang J, Yao HB, Xu AW, Yu SH. 1,3-Diamino-2-hydroxypropane-N,N,N0 ,N0-tetraacetic acid stabilized amorphous calcium carbonate: nucleation, transformation and crystal growth. Crystal Engineering Communication. 2010; 12:234–241.

49. Santos VHJM, Pontin D,Ponzi GGD, Stepanha ASG, Martel RB, Schütz MK, Einloft SMO, Vecchia FD. Application of Fourier Transform infrared spectroscopy (FTIR) coupled with multivariate regression for calcium carbonate ($CaCO_3$) quantification in cement. Construction and Building Materials. 2021; 313:125413.

50. Jungang Lv, Jimin Feng BS, Zhang W, Shi R, Yong Liu BS, Wang Z. Meng Zhao B.S.Identification of Carbonates as Additives in Pressure-Sensitive Adhesive Tape Substrate with Fourier Transform Infrared Spectroscopy (FTIR) and Its Application in Three Explosive Cases. Journal of Forensic science. 2013; 58(1):134–37.

51. Yaseen SA, Yiseen GA, Li Z. Elucidation of Calcite Structure of Calcium Carbonate Formation Based on Hydrated Cement Mixed with Graphene Oxide and Reduced Graphene Oxide. ACS Omega. 2019; 4:10160−10170.

52. Romero R, Santoyo VR, Cristina D, Sánchez M, Rosales MM. Effect of aluminum precursor on physicochemical properties of Al2O3 by hydrolysis/precipitation method. Nova Scientia. 2018; 10(20):83–99.

53. Kotwa A. Parameters of Alumina Cement and Portland Cement with Addition of Chalcedonite Meal. Materials Science and Engineering. 2017; 245:032035(1–6).

54. Liu C, Shih K, Gao Y, Li F, Wei L. Dechlorinating transformation of propachlor through nucleophilic substitution by dithionite on the surface of alumina. Journal of Soils Sediments.2012; 12:724–733.

55. Kandiban M, Vigneshwaran P, Potheher IV. Synthesis and characterization of MgO nanoparticles for photocatalytic applications. National Conference on Advances in Crystal Growwth and Nanotechnology. Conference paper. 2015.

Available: https://www.researchgate.net/publication/285525755_SYNTHESIS _AND_ CHARACTERIZATION_OF_MGO_NANOPARTICLES_FOR_PHOTOCATALYTIC_ APPLICATIONS